Acoustic nucleation of solid helium 4 on a clean glass plate

X. Chavanne, S. Balibar, and F. Caupin

Laboratoire de Physique Statistique de l'Ecole Normale Supérieure, associé aux Universités Paris 6 et Paris 7 et au CNRS, 24 rue Lhomond, 75231 Paris Cedex 05, France

We have used a focused acoustic wave to nucleate solid helium 4 on a clean glass plate. From the reflectance of light at the glass/helium interface, we measured the amplitude of the acoustic wave in the focal region. Nucleation was found to be stochastic, occurring 4.3 ± 0.2 bar above the equilibrium melting pressure. This overpressure is 2 to 3 orders of magnitude larger than found in previous nucleation studies where favorable defects or impurities must have been present. From the statistics of nucleation and its temperature dependence above 300 mK, we have estimated the activation energy E for the nucleation on the glass plate; we have found $E/k_{\mathrm{B}}T = 10$. This value is consistent with a thermally activated nucleation on a single site at the glass/helium interface. We also found a crossover to a quantum nucleation regime below 300 mK. We finally discuss some implications of these results for the homogeneous nucleation of solid helium and the search of a liquid-solid spinodal limit.

PACS numbers: 67.80.-s, 43.35.+d, 64.60.-i

1. Introduction

We recently discovered that a high intensity sound wave travelling in liquid helium 4 can crystallize it[1]. This "acoustic crystallization" is the opposite of acoustic cavitation, a phenomenon which we are studying since several years[2–4]. By focusing the wave on a glass plate, we could measure the amplitude of the density oscillation in the liquid next to the glass surface and observe the crystallization of the liquid on its path[5]. Acoustic crystallization occurs if the pressure in the wave reaches a certain threshold which we have measured. At low temperature, it is $P_{\mathrm{m}} + 4.3 \pm 0.2$ bar, where $P_{\mathrm{m}} = 25.324$

bar is the equilibrium melting pressure.

Previous studies[7] had found a much weaker metastability of liquid helium 4: solid helium 4 nucleated a few mbars only above $P_{\rm m}$. We attribute this discrepancy to the presence of highly favorable defects or impurities on the walls of the cells used in these previous experiments. Our new studies eliminate the possible presence of such favorable defects, which could be graphite particles, but, as we shall see, we have found evidence that the nucleation is still heterogeneous on one particular site of the glass surface. In section 2, we summarize our experimental methods. In section 3, we present our new results on the nucleation statistics and its temperature dependence. We have found some evidence for the existence of quantum nucleation below 300 mK. Above 300 mK, we interpret the temperature variation of the nucleation threshold as evidence for a thermally activated nucleation and we estimate the activation energy. It is consistent with thermal activation on one single site at the glass surface. We conclude with some comments about the possible observation of homogeneous nucleation and the search for a liquid-solid spinodal limit.

2. Experimental methods

As explained elsewhere[1,5], we focus 1MHz acoustic waves in liquid helium on a glass plate. The focusing produces an intense oscillation in pressure and density in a small region (0.36 mm, the acoustic wavelength) during a short time of order 1 μs. In order to measure the amplitude of the density oscillation, i.e. the exact amplitude of the acoustic wave in the focal region, we analyze the reflection of a laser beam at the glass/helium interface. Indeed, the light reflectance depends on the refractive index of helium, which is a function of its density. As a result, the reflected light is modulated by the sound wave. After a careful calibration[5], we have been able to calculate the amplitude of the sound wave from the amplitude of the reflected light. We also measured the transmission of light through the acoustic focal region. This allowed the detection of single nucleation events. These two types of measurements were done in parallel. They are illustrated in Fig. 1.

The main part of this figure shows two recordings of the light reflected at the glass/helium interface. One recording corresponds to an excitation voltage of 8.45 V on the piezoelectric transducer. It shows a nearly sinusoidal acoustic wave. Superimposed on it is a recording at a slightly higher voltage (8.55 V) where the density is modified by the nucleation of solid helium. These two recordings are averages over 10 000 acoustic bursts. For the one at 8.45 V, a selective average is done on the signals with no nucleation only.

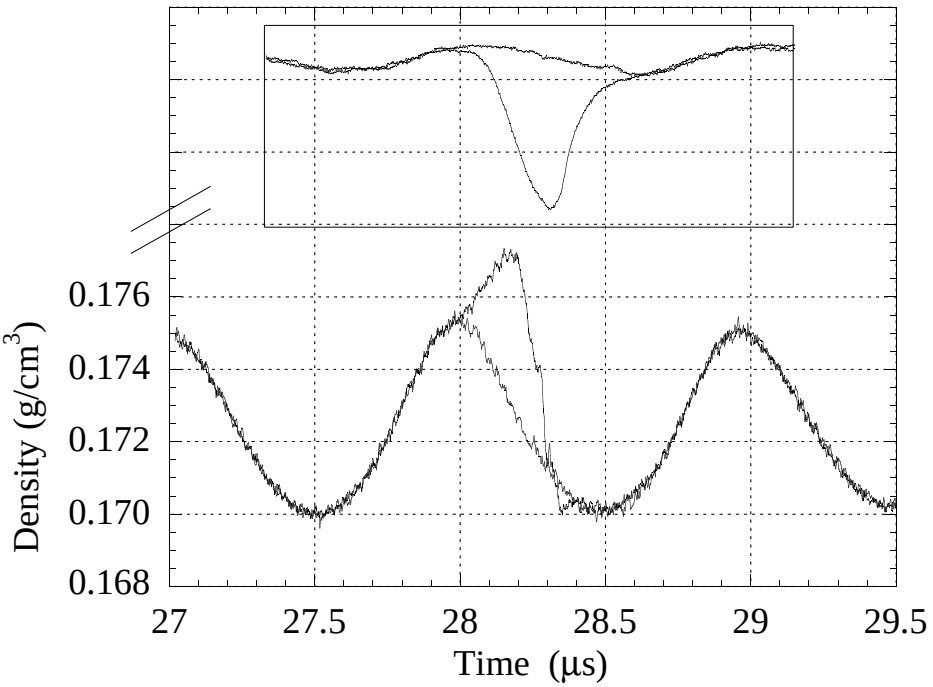

Fig. 1. The main part of the figure shows two superimposed recordings of the helium density at the glass/helium interface. They were obtained by analyzing the reflection of light. One recording shows the acoustic wave only; the other shows the effect of the nucleation of crystals. In the inset on top, two other recordings are also superimposed. The vertical axis is now the intensity of the light transmitted through the acoustic focal region (in arbitrary units). One recording shows a modulation by the acoustic wave only while the other shows a large negative signal due to one nucleation event. By counting traces of one kind or the other, we measured the nucleation probability (see text).

We used it to determine the nucleation threshold density. For the one at 8.55 V, it is not a selective average, nearly all signals showing nucleation.

In the inset on top, two other recordings are also superimposed; the horizontal axis is the same as in the main part of the figure (time) but the vertical one is the intensity of the light transmitted through the acoustic focal region (in arbitrary units). They are now single traces obtained without averaging. They have been recorded with the same voltage (8.45V) and they show the stochastic character of nucleation. The first trace is nearly sinusoidal and corresponds to the small scattering from the acoustic wave only. For this excitation voltage, 45% of the transmitted signals were like

this (no nucleation event). The second trace shows a large negative peak due to the nucleation of a crystal. 55 % of the traces were like this second one. Since it is easy to discriminate between these two kinds of transmitted signals, such recordings allowed us to measure the nucleation probability for each excitation level.

In the presence of a crystal, the reflected light is sensitive to the contact area of this crystal to the glass plate, while the transmitted signal measures the size of the crystal. This probably explains why the nucleation is detected at the same time, the wave maximum, on the two signals, but the reflected signal ends earlier than the transmitted signal. We are currently working on a quantitative analysis of the growth and melting dynamics of our crystals, which are very fast at low temperature. Above 1K, the crystals are more difficult to detect, presumably because they grow up to a smaller size, their growth dynamics being slower[6].

The transducer is excited at its resonance frequency (1.019 MHz) during six periods (about 6 μs) only. Since its quality factor Q is about 50, the amplitude of the emitted wave increases during the first six periods and decreases slowly afterwards. The maximum pressure is reached at the seventh positive swing. A lens of focal length 22 mm is located inside the experimental cell and focuses an Ar^+ laser beam onto the acoustic focal region. Our spatial resolution is fixed by the size of the laser spot at the optical focus; it is 14 μm, i.e. small compared to the acoustic wavelength. We detect the ac-modulation of the reflected light with an avalanche photodiode. Thanks to a fast digital oscilloscope our time resolution is 10 ns.

For the conversion of densities ρ into pressures P or the reverse, we have used the following equation of state:

$$\rho = 0.094262 \; + \; 0.0239105(P + 9.6201)^{1/3} \tag{1}$$

with pressures in bars and densities in g/cm^3. This is the same form as what H.J. Maris[8] used at negative pressure but the numbers are slightly different because, for the present purpose, we fitted the cubic law on the high pressure data of Abraham et al.[9]. At high pressure, this equation of state is simple to invert and almost undistinguishable from the similar cubic law of Abraham himself[9]. In this region of the phase diagram, the equation of state is known with an accuracy of about 10^{-5}g/cm^3 in density, 0.02 bar in pressure.

In order to improve the signal to noise ratio on the reflected beam, we averaged on about 10000 signals repeated at 1 to 10 Hz. As one can see in Fig. 1, the sensitivity of our measurement is of order $10^{-4}\ g/cm^3$ for the absolute density, or equivalently 0.2 bar. For the analysis of the nucleation statistics, we are interested in density differences, which are known with a smaller uncertainty, about $10^{-5} g/cm^3$. No averaging was necessary for the

detection of the transmitted light which is intense and strongly scattered by the nucleation of crystals.

The signals shown in Fig. 1 were recorded at 602 mK, with a static pressure $P_{\rm stat}$ in the cell equal to the equilibrium melting pressure $P_{\rm m}$. This means that there was some solid helium in the bottom part of the cell; the transducer, the glass plate and the lens were all in the liquid above. In these conditions, the crystals grew larger and were easier to detect than if we worked at a lower static pressure. However, with this setup, we could study nucleation and obtain similar results at any static pressure from 0 to $P_{\rm m}$ in the range from 30 mK to 1.5 K.

3. Nucleation: statistics and temperature dependence

As usual, we observed that the nucleation of solid helium is a stochastic phenomenon. It is most easily seen from the light transmitted through the acoustic focus, as shown in the inset of Fig. 1. With such signals, our digital oscilloscope easily discriminated bursts which led to nucleation from others which did not. A computer automatically counted nucleation events in series of 500 bursts which were repeated at a rate of a few Hertz. It calculated the nucleation probability as a function of the maximum density reached in the acoustic wave (see Fig. 2). This density was obtained from the calibration of the sound amplitude at the focus as a function of the excitation voltage.

The solid line in Fig. 2 is a fit of the data points with the equation:

$$\Sigma = 1 - \exp\left(-\Gamma_0 \exp\left(-\frac{E}{T}\right)\right) = 1 - \exp\left(-\ln 2 \exp\left(b\,\frac{\rho-\rho_{\rm c}}{\rho_{\rm c}}\right)\right) \qquad (2)$$

where Σ is the nucleation probability and the activation energy E has been expanded to first order around $E(\rho_{\rm c})$. Γ_0 is a prefactor which will be discussed below. The above equation leads to an "asymmetric S-shape" curve with an inverse width b given by

$$b = \frac{\rho_{\rm c}}{T}\frac{\partial E}{\partial \rho} \qquad (3)$$

Fig. 2 shows data obtained at the same 602 mK as for Fig. 1. When starting from a lower static pressure (10 to 25 bar), we found the same nucleation density $\rho_{\rm c}$ with a larger sound amplitude. From the above equation of state, it is easily converted into a nucleation pressure. We also checked that the nucleated crystal was hcp helium. This was done by increasing the sound amplitude much more. We observed a saturation of the reflected signal at 0.19 g/cm^3, the density of hcp solid helium.

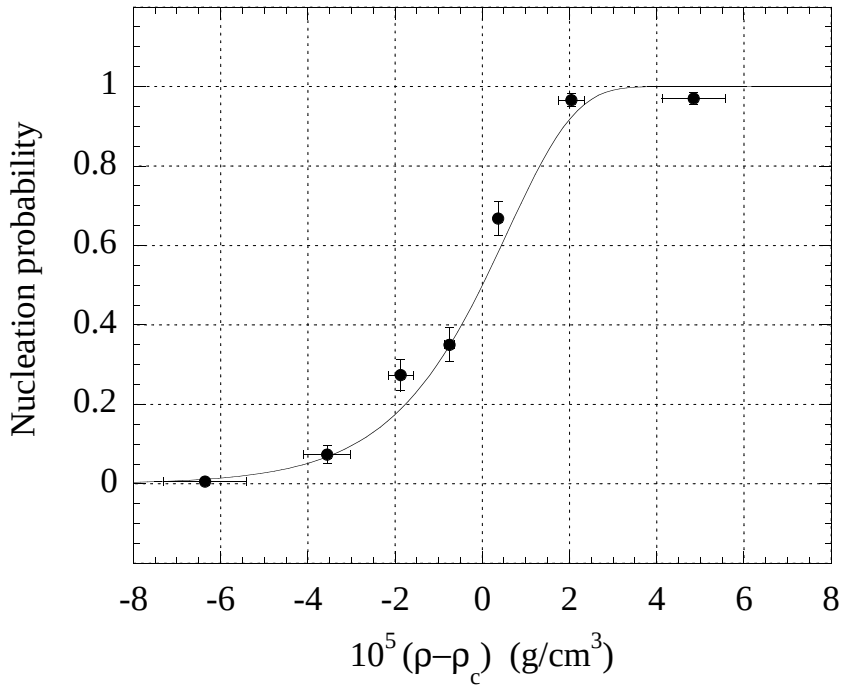

Fig. 2. The nucleation probability as a function of the liquid helium density ρ ($\rho_c = 0.17543$ g/cm^3 is the threshold density where the nucleation probability is 0.5). The solid line corresponds to a simple model of thermally activated nucleation (Eq. (2), see text). Data taken at 602 mK with the cell at the equilibrium melting pressure, i.e. a static density $\rho_{\rm stat} = \rho_{\rm m} = 0.17245$ g/cm^3. The nucleation probability increases continuously from zero to one in a narrow density interval.

The fit with Eq. (2) determines the value $b = -11200 \pm 1000$, which gives us the density dependence of the activation energy:

$$\frac{\partial E}{\partial \rho} = -3.84 \times 10^4 \,\mathrm{Kcm^3/g}. \tag{4}$$

In order to obtain the activation energy itself, we need to study the temperature variation of the nucleation density. Indeed, since most of the temperature dependence of the nucleation probability is due to the Arrhenius factor in Eq. (2), the quantity E/T is roughly constant along the nucleation curve $\rho_c(T)$. Taking its temperature derivative leads to the equation

$$\frac{E}{T} = \frac{\partial E}{\partial \rho}\frac{\partial \rho_c(T)}{\partial T} \tag{5}$$

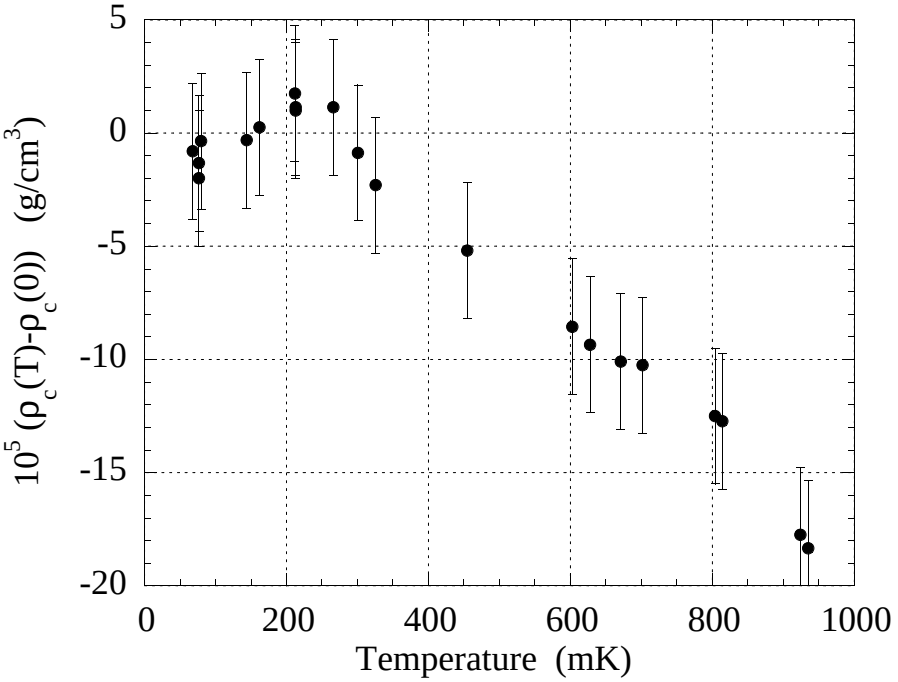

Fig. 3. The temperature dependence of the nucleation threshold density $\rho_c(T)$. In the low temperature limit, the threshold tends to $\rho_c(0) = 0.17552 \pm 0.00010 g/cm^3$. The decrease above 300 mK is typical of a thermally activated regime. The nearly constant value below 300 mK is a strong indication of a crossover to quantum nucleation below this temperature.

if we neglect a small possible dependence of the relation $E(\rho)$ on T. As shown in Fig. 3, we have also measured the temperature dependence of the threshold density ρ_c. This figure shows the existence of a temperature independent regime below 300 mK, which is likely to correspond to nucleation by quantum tunneling. In the low temperature limit, the nucleation threshold tends to $\rho_c(0)$=0.17552 $\pm$ 0.00010 g/cm^3, a density which corresponds to $P_c = P_m + 4.3 \pm 0.2$ bar. Above the crossover temperature 300 mK, the nucleation threshold decreases as expected for a thermally activated nucleation. The slope of this classical regime is

$$\frac{\partial \rho_c}{\partial T} = -2.6 \times 10^{-4}\, \mathrm{gcm^{-3}K^{-1}} \qquad (6)$$

From Eqs. (4), (5) and (6), we conclude that the activation energy is $E/T = 10$ along the nucleation curve. This value is consistent with a nucleation on a single defect. Indeed, the prefactor $\Gamma_0 = \nu\eta\tau$ is the product of an attempt frequency ν by a number η of independent nucleation sites

and by the experimental time τ. In a non-dissipative medium such as superfluid helium[2], the attempt frequency ν is a typical frequency of thermal fluctuations, of order $k_{\rm B}T/\hbar \approx 10^{11}\,$Hz. As for τ, it is the time during which there is a significant probability of nucleation, typically 0.1 μs, a fraction of the sound period[2]. With these values, we can estimate the number η of nucleation sites from the equation

$$\Gamma_0 = \nu\eta\tau = \ln(2) \times \exp\left(\frac{E}{T}\right) \tag{7}$$

and we find $\eta \approx 1$. If we had homogeneous nucleation on the glass surface, this density would be equal to the size of the acoustic focal region divided by the typical size of the critical nucleus, a much larger number of order 10^7. We thus conclude that, in this experiment, nucleation takes place on one single defect, the most favorable one in the acoustic focal region.

What is the nature of this defect? As explained in Ref. 1, homogeneous nucleation could not happen 4.3 bars above $P_{\rm m}$: the activation energy would be about 3000K and the corresponding nucleus would have a radius of order 100 Å. This is too large. Since the contact angle of the solid-liquid interface with usual walls is 45 degrees [12,13], the nucleation is more likely to take place on the glass plate than in the bulk, although the glass wall is more favorable to the liquid. However, a nucleus in the shape of a truncated sphere, touching a flat wall with a 45 degrees angle, would have an energy only slightly lower than a full sphere in the bulk. Our finding of an activation energy of order 10K indicates that the geometry of this defect is particular. Can it be a 100 Å cavity? Is the reduction of the energy barrier a simple consequence of the van der Waals field in this cavity ? These interesting questions need further study.

4. Conclusions

Heterogeneous nucleation is not an easy subject to study, because the exact nature of the nucleation site is rarely known. From our present results it is still possible to draw several conclusions. Balibar, Mizusaki and Sasaki[14] had proposed that, in ordinary cells, solid helium nucleates a few mbars only above $P_{\rm m}$, on favorable defects which might be graphite particles. The present method eliminates the possible presence of such defects in the small acoustic focal region, so that we find a much larger overpressure, about 4.3 bar. However, we have found that the nucleation still takes place on a wall defect whose nature is unknown. We have also found a crossover to a temperature independent nucleation regime below 300 mK, which is likely to result from quantum tunneling. Our results are also promising

for the search for homogeneous nucleation of solid helium. From the light transmitted through the acoustic focus, we have shown that it is easy to detect the nucleation of solid helium, at least below 1K, and removing the glass plate should not change our sensitivity. We are thus searching for homogeneous nucleation at even higher overpressure. We have already found that, in the absence of walls, helium can stay liquid up to $P_{\rm m}$ + 17 bar. We expect to see homogeneous nucleation below 100 bar. This is where we locate the possible existence of a liquid/solid spinodal limit, which should correspond to the vanishing of the roton gap. Indeed, the roton gap is a measure of the local order of liquid helium. When the roton becomes soft, a density modulation should spontaneously appear in the liquid which should thus be totally unstable against the formation of the solid. We hope to find experimental evidence for this phenomenon and to be able to compare with possible calculations[15] of the critical pressure (or density) where the roton gap vanishes.

REFERENCES

1. X. Chavanne, S. Balibar, F. Caupin, *Phys. Rev. Lett.* **86**, 5506 (2001).
2. H. Lambaré, P. Roche, S. Balibar, H.J. Maris, O.A. Andreeva, C. Guthmann, K.O. Keshishev and E. Rolley, *Eur. Phys. J. B* **2**, 381 (1998).
3. F. Caupin and S. Balibar, *Phys. Rev. B* **64**, 064507 (2001); F. Caupin, S. Balibar and H.J. Maris, *Phys. Rev. Lett.* **87**, 145302 (2001).
4. X. Chavanne, S. Balibar and F. Caupin, *Proc. of QFS2001*, to appear in *J. Low Temp. Phys.* (2001).
5. X. Chavanne, S. Balibar, F. Caupin, C. Appert and D. d'Humières, *Proc. of QFS2001*, to appear in *J. Low Temp. Phys.* (2001).
6. K.O. Keshishev, A.Ya. Parshin and A.B. Babkin, *Zh. Eksp. Teor. Fiz.* **80**, 716 (1981) [*Sov. Phys. JETP* **53**, 362 (1981)]; J. Bodensohn, K. Nicolai and P. Leiderer, *Z. Phys. B* **64**, 55 (1986); S. Balibar, D.O. Edwards and W.F. Saam, *J. Low Temp. Phys.* **82**, 119 (1991).
7. S. Balibar, B. Castaing and C. Laroche, *J. Phys. (Paris) Lett.* **41**, 283 (1980); V.L. Tsymbalenko, *J. Low Temp. Phys.* **88**, 55 (19); J.P. Ruutu, P.J. Hakonen, J.S. Penttila, A.V. Babkin, J.P. Saramaki and E.B. Sonin, *Phys. Rev. Lett.* **77**, 2514 (1996); Y. Sasaki and T. Mizusaki, *J. Low Temp. Phys.* **110**, 491 (1998); T.A. Johnson and C. Elbaum, *Phys. Rev.* **E 62**, 975 (2000).
8. H.J. Maris, *Phys. Rev. Lett.* **66**, 45 (1991).
9. B.Abraham, Y. Eckstein, J.B. Ketterson, M. Kuchnir and P.R. Roach, *Phys. Rev.* **A1**, 250 (1970).
10. C. Appert, X. Chavanne, S.Balibar, D. d'Humières and C. Tenaud, *Rencontres du Non-Linéaire 2001*, Paris Onze Editions, Uni. Paris Sud (march 2001), and to be published.
11. J.W. Beams, *Phys. Rev.* **104**, 880 (1956); R.D. Finch, R. Kawigada, M. Barmatz and I. Rudnick, *Phys. Rev.* **134**, A1425 (1964); P.D. Jarman and K.J. Taylor,

J. Low Temp. Phys. **2**, 389 (1970); P.L. Marston, *J. Low Temp. Phys.* **25**, 383 (1975).
12. K.O. Keshishev, A.Ya. Parshin and A.V. Babkin, *Pis'ma Zh. Eksp. Teor. Fiz.* **30**, 63 (1979) (*Sov. Phys. JETP Lett.* **30**, 56 (1979)).
13. E.Rolley, C. Guthmann, E. Chevalier and S.Balibar , *J. Low Temp. Phys.* **99**, 851 (1995).
14. S. Balibar, T. Mizusaki and Y. Sasaki, *J. Low Temp. Phys.* **120**, 293 (2000).
15. T. Minoguchi, Proc. of QFS2001, to appear in *J. Low Temp. Phys.* (2001).